Direct printing of aligned carbon nanotube patterns for high-performance thin film devices

Jiwoon Im,[1,2] Il-Ha Lee,[2,3] Byung Yang Lee,[1] Byeongju Kim,[1] June Park,[4] Woojong Yu,[2,3] Un Jeong Kim,[2] Young Hee Lee,[3] Maeng-Je Seong,[4] Eun Hong Lee,[2,a)] Yo-Sep Min,[5,b)] and Seunghun Hong[1,c)]

[1]*Department of Physics and Astronomy, Seoul National University, Seoul 151-747, Republic of Korea*
[2]*Frontier Research Laboratory, Samsung Advanced Institute of Technology, Yongin, Gyeonggi-Do 449-712, Republic of Korea*
[3]*Department of Physics, Center for Nanotubes and Nanostructured Composites, Sungkyunkwan Advanced Institute of Technology, Sungkyunkwan University, Suwon 440-746, Republic of Korea*
[4]*Department of Physics, Chung-Ang University, Seoul 156-756, Republic of Korea*
[5]*Department of Chemical Engineering, Konkuk University, Seoul 143-701, Republic of Korea*

(Received 1 September 2008; accepted 20 December 2008; published online 3 February 2009)

The aligned assembly of carbon nanotubes (CNTs) on substrate presents a significant bottleneck in the fabrication of high-performance thin film devices. Here, we report a direct printing method to prepare *laterally aligned thick* CNT patterns over *large* surface regions. In this method, CNT forests were grown selectively on specific regions of one substrate, and the forest patterns were transferred on another SiO_2 substrate in a laterally aligned formation while keeping their original shapes. The degree of alignment was characterized via electrical measurement and polarized Raman spectroscopy. Furthermore, we demonstrated high-performance field-effect transistors and gas sensors using our method. © *2009 American Institute of Physics*. [DOI: 10.1063/1.3073748]

Thin film devices based on single-walled carbon nanotube (swCNT) were extensively studied for various applications.[1–5] Previous successful assembly methods for such devices included selective growth, surface-programed assembly, direct transfer, etc.[6–17] However, previous methods usually allowed us to prepare monolayer patterns of swCNTs, and it is still considered to be very difficult to prepare multiple layer of laterally aligned swCNTs. Here, we report a method to directly print *laterally aligned thick* CNT patterns over *large* surface area on solid substrates. In this process, swCNTs were grown vertically on specific regions of one substrate, and the vertically grown swCNT patterns were transferred onto another SiO_2 substrate in a laterally aligned formation while keeping their original shapes. As a proof of concepts, we demonstrated high-performance field-effect transistors (FETs) and gas sensors using our method.

Figure 1 depicts our assembly method. The first step comprises the patterning of catalyst films for selective swCNT growth [Fig. 1(a)]. Here, aluminum thin films (20 nm) were deposited on glass wafer by thermal evaporation and oxidized at 600 °C in air to form alumina film.[18] Then, Fe films (~0.5 nm) were deposited via e-beam evaporation and thermally oxidized at 600 °C for 10 min in air. The photoresist was patterned on the film by photolithography, and the exposed area of the film was etched by buffered oxide etching process to prepare the catalyst patterns [Fig. 1(a)]. Then, swCNTs were grown vertically on the catalyst patterns using a homebuilt radio-frequency remote-plasma chemical vapor deposition system with water vapor [Fig. 1(b)].[18,19] The substrate with vertically grown swCNT patterns (*donor* substrate) was faced down against a SiO_2 substrate (*acceptor* substrate) and sled ~1 mm to a certain direction with ~5 kPa of downward pressure [Figs. 1(c) and 1(d)]. During the printing process, swCNTs were transferred to the SiO_2 substrate with the alignment along the sliding direction, forming laterally aligned thick swCNT film patterns [Fig. 1(e)]. Since the swCNT films form a stable structure, we can continue the microfabrication process to build additional device structures such as electrodes (30 nm Au on 10 nm Ti) [Fig. 1(f)].

Figures 2(a) and 2(b) show the donor and acceptor substrates, respectively. Note that the transferred swCNT patterns on the acceptor substrate maintained their original pattern shapes [Fig. 2(b)]. The linewidth of printed CNT film was larger than that of the CNT forest patterns by only ~5%. When we used the swCNT forest patterns with ~10 μm height, we achieved printed CNT film with ~3 μm thickness, indicating that the angle between the printed swCNTs

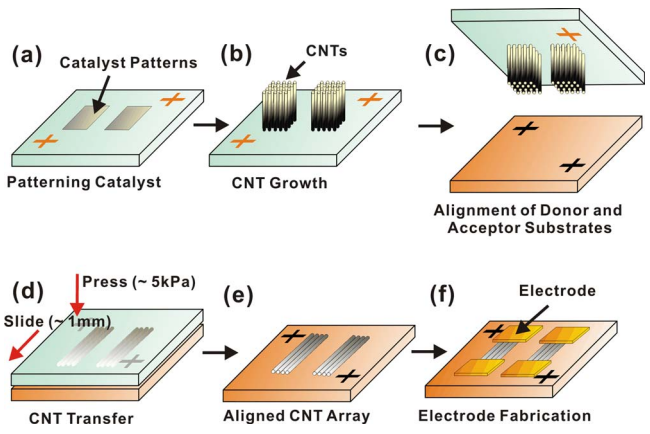

FIG. 1. (Color online) Schematic diagram depicting the direct-printing method of laterally aligned swCNTs. (a) Patterning catalyst film (Al 20 nm/Fe 0.5 nm) on a glass substrate. (b) Vertical growth of swCNTs. (c) Placing the vertically grown swCNT forest patterns (donor substrate) onto a SiO_2 substrate (acceptor substrate). (d) Application of pressure and sliding of the donor substrate against the acceptor substrate. (e) Laterally aligned swCNT patterns on the acceptor substrate after the removal of donor substrate. (f) Electrode fabrication.

a)Electronic mail: elee@samsung.com.
b)Electronic mail: ysmin@konkuk.ac.kr.
c)Electronic mail: seunghun@snu.ac.kr.

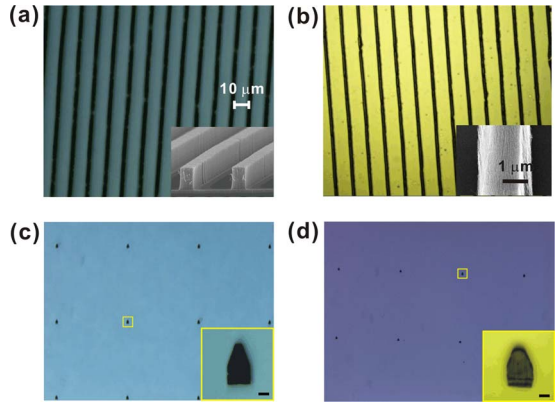

FIG. 2. (Color online) (a) 2 μm linewidth (10 μm gap) patterns of swCNT forest grown vertically on a glass substrate. (The inset shows the scanning electron microscopy image of the swCNT forest.) (b) Printed swCNTs on the SiO_2 substrate from the sample in (a). (c) Dot shaped swCNT forest pattern array on glass substrate. (d) Printed swCNTs on SiO_2 substrate from the sample in (c). Scale bars in (c) and (d) represent 10 μm.

and the substrate was ~17.5°. The energy-dispersive x-ray spectroscopy on the printed swCNT patterns exhibited minor Al trace (~1%) (Fig. S1 in the supplemental material),[20] implying that some of the detached CNTs were decorated with FeO_x/AlO_x catalyst. However, the donor substrate still retained the majority of the catalytic film so that we could reuse the donor substrate for additional swCNT growth after printing. We could also achieve similar *dot shaped* swCNT patterns [Figs. 2(c) and 2(d)]. The printed pattern width in the perpendicular direction to the sliding was increased by ~1.5 μm due to the spreading by downward pressure, and that in the parallel direction was decreased by ~0.5 μm by compressive stacking.

The printed swCNT films exhibited highly anisotropic electrical properties due to the lateral alignment of swCNTs. We printed cross shaped swCNT patterns and measured the directional resistance values, revealing the anisotropic electrical properties of the printed swCNT films [Fig. 3(a)].[21]

We utilized polarized Raman method to further characterize the CNT alignment in the printed film.[22] At first, we took the Raman spectra using 514.5 nm line from an Ar^+ laser as the excitation light source in two polarization configurations, where both the incident and the scattered photons were polarized parallel (blue curve) or normal (red curve) to the line-pattern direction [Fig. 3(b)]. According to the Raman scattering selection rule, the Raman scattering intensity I from an individual CNT depends on the polarization angle of the light as $I \sim \cos^4 \theta$, where θ represents the angle between the polarization of light and the alignment of the CNT.[23] Our results show that the G-band (~1590 cm^{-1}) intensity by the light polarized *parallel* (I_P) to the CNT direction is ~3.7 times larger than that by the light polarized *normal* (I_n) to the CNTs, indicating a high-degree alignment of CNTs along the sliding direction.[22]

For detailed analysis, we measured polarized Raman spectra using the light with several polarization directions [Fig. 3(c)]. Here, the G-band intensity by the light with a specific polarization direction was normalized to that for the parallel polarization configuration (θ=0). The angular distribution of CNTs in the printed structures was estimated from the normalized G-band intensity data via a simple calculation after assuming that the *Gaussian* angular distribution of CNTs and the Raman intensity relation $I \sim \cos^4 \theta$ for individual CNTs in the printed structure [Fig. 3(d)].[24] The results indicate Gaussian angular distribution of CNTs with full width at half maximum ~48°.

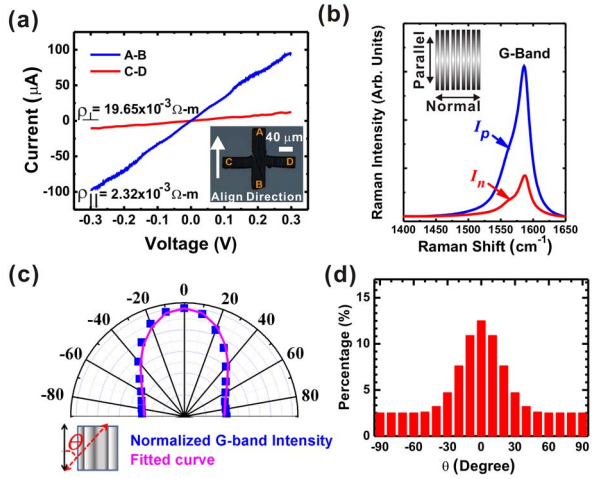

FIG. 3. (Color online) (a) Directional I-V characteristics of "cross shaped" printed swCNT patterns. The blue or red lines represent the results measured between A and B or C and D points, respectively. (b) Polarized Raman spectra of the CNT G-band. The blue line is for the vertically polarized incident and scattered photons (parallel to printing direction) and the red line for the horizontally polarized photons (normal to printing direction). (c) The angular dependence of the G-band polarized Raman intensity normalized to that for the parallel polarization configuration, where θ=0. (d) Estimated Gaussian angular distribution of swCNTs from the experimental data of the normalized G-band Raman intensity for the measured polarization angles.

In some applications such as sensors, it is desirable to prepare a single layer of swCNTs [Fig. 4(a)]. We placed the printed swCNTs in *o*-dichlorobenzene and applied ultrasonic vibration with 30 W power for 5 s to remove most of swCNTs and prepare swCNT monolayer. In *o*-dichlorobenzene, the adhesion forces between swCNTs and SiO_2 surface were stronger than those between swCNTs,[9,11,25] and we could remove most of the swCNTs. The average length of the swCNTs on the monolayer film was found to be ~2.5 μm. It was a bit shorter than the original lengths of the swCNTs. Presumably, rather long swCNTs were broken into small pieces by ultrasonic vibration [Fig. S2 in the supplemental material].[20,26] Our control

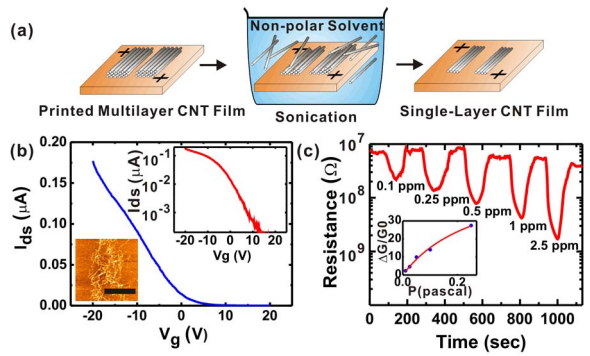

FIG. 4. (Color online) Preparation of a monolayer pattern of swCNTs for the fabrication of high-performance FETs and gas sensor. (a) Schematic diagram depicting the method to prepare swCNT monolayer patterns from laterally aligned thick swCNT films. (b) Gating effect of a high-performance FET based on swCNT monolayer patterns. (The inset shows the log plot of the gating effect and atomic force microscopy image.) (c) Response of swCNT monolayer devices to the exposure of NO_2 gas. The inset shows the response $\Delta G/G_0$ vs partial pressure p, where ΔG is the change in conductance with respect to initial conductance G_0.

experiments show that rather long swCNTs (~10 μm long) were easily broken into small pieces (~2 μm long) by ultrasonic treatment. However the breaking process slowed down after the fragmentation of the long swCNTs. Thus, we could still build various devices such as FETs and sensors using this process.

We demonstrated the high-performance FETs based on the swCNT monolayer patterns [Fig. 4(b) and Fig. S3 in the supplemental material].[20] Since our swCNT networks include metallic swCNTs, some metallic paths in the network may result in poor on-off ratio. To achieve high-performance FETs with a large on-off ratio, the density of swCNT networks was lowered down to a single monolayer by ultrasonic treatment.[27,28] When the swCNT density in the swCNT networks was low, it was more likely that only semiconducting paths were formed because there were usually more semiconducting swCNTs than metallic ones. Figure 4(b) shows the typical characteristics of our FETs based on swCNT monolayer films. Our FETs exhibited a *p -type* behavior with the on-off ratio of $\sim 10^4$.[29] Although swCNTs have ambipolar properties, it was reported that swCNT-based FETs in air exhibited *p*-type characteristics because oxygen molecules adsorbed onto the swCNTs retrieved electrons and left only hole carries in the swCNTs. The carrier mobility was estimated ~9.9 C m^2/V s using classical mobility equation

$$\mu = (dI_{sd}/dV_G)(L^2/C_g)(1/V_{sd}). \quad (1)$$

Here, L and C_g represent the channel length and gate capacitance, respectively. The gate capacitance was calculated using parallel plate model[30] and Fig. S4 (supplemental material).[20]

Figure 4(c) shows the response of a gas sensor based on swCNT monolayer film. The resistance was observed to decrease when exposed to NO_2 gas diluted in N_2. It was reported that one can achieve the maximum detection sensitivity using monolayer films of swCNTs.[28] Our gas sensors based on swCNT monolayer patterns exhibited high sensitivity to NO_2 gas without any other treatments even at room temperature. The sensor response results can be modeled as in previous report.[31] In brief, we assumed that the sensor response $\Delta G/G_0$ follows $\Delta G/G_0 \propto \theta$ at low concentration NO_2 gas, where G_0, ΔG, and θ represent initial conductance, conductance change, and the coverage of NO_2 onto CNT surfaces, respectively. By applying Langmuir isotherm model, the sensor response $\Delta G/G_0$ to NO_2 can be written as

$$\Delta G/G_0 \propto 1/\{1 + [(2\pi m k_B T)^{1/2} v \exp(-E_b/k_B T)]/pS\sigma\}. \quad (2)$$

The sensor response results were fitted to estimate the sticking coefficient $S \sim 5.75 \times 10^{-5}$ at room temperature using the values from Ref. 31 for all other parameters [Fig. 4(c), inset].

In summary, we presented a strategy to mass-produce laterally aligned thick swCNTs patterns over large surface area. The optical and electrical analysis revealed high degree of swCNT alignment and anisotropic electrical properties of the printed swCNT films. Furthermore, we prepared swCNT monolayer films using the ultrasonication step, which enabled the fabrication of high-performance FETs and sensitive gas sensors. This is a simple but versatile method to directly print laterally aligned thick and monolayer swCNT films and should open up various device applications based on swCNTs.

This project has been supported by TND program. M.S. acknowledges support by the Korean Science and Engineering Foundation (KOSEF) (Grant No. R01-2006-000-10883-0) and by Seoul R&BD Program (Grant No. 10550). S.H. acknowledges partial support from NRL program (Grant No. R0A-2004-000-10438-0) of KOSEF and Ecotechnopia 21 project of KME.

[1] S. J. Tans, R. M. Verschueren, and C. Dekker, Nature (London) **393**, 49 (1998).
[2] R. Martel, T. Schmidt, H. R. Shea, T. Hertel, and Ph. Avouris, Appl. Phys. Lett. **73**, 2447 (1998).
[3] Y. Cui, Q. Wei, H. Park, and C. M. Lieber, Science **293**, 1289 (2001).
[4] S. Ghosh, A. K. Sood, and N. Kumar, Science **299**, 1042 (2003).
[5] A. Javey, J. Guo, Q. Wang, M. Lundstrom, and H. Dai, Nature (London) **424**, 654 (2003).
[6] Y. Huang, X. F. Duan, Q. Q. Wei, and C. M. Lieber, Science **291**, 630 (2001).
[7] R. Krupke, F. Hennrich, H. Lohneysen, and M. M. Kappes, Science **301**, 344 (2003).
[8] J. Liu, M. J. Casavant, M. Cox, D. A. Walters, P. Boul, W. Lu, A. J. Limberg, K. A. Smith, D. T. Colbert, and R. E. Smalley, Chem. Phys. Lett. **303**, 125 (1999).
[9] S. G. Rao, L. Huang, W. Setyawan, and S. Hong, Nature (London) **425**, 36 (2003).
[10] N. Nuraje, I. A. Banerjee, R. I. MacCuspie, L. Yu, and H. Matsui, J. Am. Chem. Soc. **126**, 8088 (2004).
[11] M. Lee, J. Im, B. Y. Lee, S. Myung, J. Kang, L. Huang, Y.-K. Kwon, and S. Hong, Nat. Nanotechnol. **1**, 66 (2006).
[12] S. Myung, M. Lee, G. T. Kim, J. S. Ha, and S. Hong, Adv. Mater. (Weinheim, Ger.) **17**, 2361 (2005).
[13] S. Y. Park, S. Y. Park, S. Namgung, B. Kim, J. Im, J. Y. Kim, K. Sun, K. B. Lee, J.-M. Nam, Y. Park, and S. Hong, Adv. Mater. (Weinheim, Ger.) **19**, 2530 (2007).
[14] J. Kang, J. Lee, T. H. Kim, J. Park, M.-J. Seong, and S. Hong, Nanotechnology **19**, 135305 (2008).
[15] C. Zhou, J. Kong, E. Yenilmez, and H. Dai, Science **290**, 1552 (2000).
[16] S. J. Kang, C. Kocabas, H.-S. Kim, Q. Cao, M. A. Meitl, D.-Y. Khang, and J. A. Rogers, Nano Lett. **7**, 3343 (2007).
[17] Z. Fan, J. C. Ho, Z. A. Jacobson, R. Yerushalmi, R. L. Alley, H. Razavi, and A. Javey, Nano Lett. **8**, 20 (2008).
[18] I. H. Lee, J. Im, E. J. Bae, K.-K. Kim, E. H. Lee, Y. H. Lee, S. Hong, and Y.-S. Min, "Low temperature growth of single-walled carbon nanotube forest" (unpublished).
[19] Y.-S. Min, E. J. Bae, B. S. Oh, D. Kang, and W. Park, J. Am. Chem. Soc. **127**, 12498 (2005).
[20] See EPAPS Document No. E-APPLAB-94-038904 for supplementary experimental data. For more information on EPAPS, see http://www.aip.org/pubservs/epaps.html.
[21] C. Kocabas, S.-H. Hur, A. Gaur, M. A. Meitl, M. Shim, and J. A. Rogers, Small **1**, 1110 (2005).
[22] J. Park, M. J. Seong, J. Im, M. Lee, S. Hong, H. C. Cho, K. M. Kim, and H. Cheong, J. Korean Phys. Soc. **48**, 1347 (2006).
[23] H. H. Gommans, J. W. Alldredge, H. Tashiro, J. Park, J. Magnuson, and A. G. Rinzler, J. Appl. Phys. **88**, 2509 (2000).
[24] J. Park, M. J. Seong, J. Im, M. Lee, S. Myung, S. Hong, K. M. Kim, and H. Cheong, "Polarized Raman study of carbon nanotubes adsorbed onto line-patterned substrates" (unpublished).
[25] J. Im, L. Huang, J. Kang, M. Lee, D. J. Lee, S. G. Rao, N.-K. Lee, and S. Hong, J. Chem. Phys. **124**, 224707 (2006).
[26] J. Hilding, E. A. Grulke, Z. G. Zhang, and F. Lockwood, J. Dispersion Sci. Technol. **24**, 1 (2003).
[27] C. Kocabas, N. Pimparkar, O. Yesilyurt, S. J. Kang, M. A. Alam, and J. A. Rogers, Nano Lett. **7**, 1195 (2007).
[28] V. Skákalová, A. B. Kaiser, Y.-S. Woo, and S. Roth, Phys. Rev. B **74**, 085403 (2006).
[29] V. Derycke, R. Martel, J. Appenzeller, and Ph. Avouris, Appl. Phys. Lett. **80**, 2773 (2002).
[30] S. J. Kang, C. Kocabas, T. Ozel, M. Shim, N. Pimparkar, M. A. Alam, S. V. Rotkin, and J. A. Rogers, Nat. Nanotechnol. **2**, 230 (2007).
[31] P. Qi, O. Vermesh, M. Grecu, A. Javey, Q. Wang, H. Dai, S. Peng, and K. J. Cho, Nano Lett. **3**, 347 (2003).